JOURNAL OF VIROLOGY, Nov. 2011, p. 11159–11169 Vol. 85, No. 21
0022-538X/11/$12.00 doi:10.1128/JVI.00720-11

Mechanism of Glycyrrhizic Acid Inhibition of Kaposi's Sarcoma-Associated Herpesvirus: Disruption of CTCF-Cohesin-Mediated RNA Polymerase II Pausing and Sister Chromatid Cohesion▽

Hyojeung Kang[1,2] and Paul M. Lieberman[1]*

The Wistar Institute, Philadelphia, Pennsylvania 19104,[1] and Kyungpook National University, Daegu, South Korea[2]

Received 8 April 2011/Accepted 22 August 2011

Glycyrrhizic acid (GA), a derivative of licorice, selectively inhibits the growth of lymphocytes latently infected with Kaposi's sarcoma-associated herpesvirus. The mechanism involves the deregulation of the multicistronic latency transcript, including the failure to generate the mature forms of viral mRNA encoding LANA. We show here that GA disrupts an RNA polymerase II (RNAPII) complex that accumulates at the CTCF-cohesin binding site within the first intron of the latency transcript. GA altered the enrichment of the RNAPII pausing complex, along with pausing factors SPT5 and NELF-A, at the intragenic CTCF-cohesin binding sites. GA blocked the interaction of cohesin subunit SMC3 with another cohesin subunit, RAD21, and reduced SPT5 interaction with RNAPII. Covalent coupling of GA to a solid support revealed that GA interacts with several cellular proteins, including SMC3 and SPT5, but not their respective interaction partners RAD21 and RNAPII. GA treatment also inhibited the transcription of some cellular genes, like c-*myc*, which contain a similar CTCF-cohesin binding site within the first intron. We also found that GA leads to a more general loss of sister chromatid cohesion for cellular chromosomes. These findings suggest that RNAPII pauses at intragenic CTCF-cohesin binding sites and that abrogation of this pausing by GA leads to loss of proper mRNA production and defects in sister chromatid cohesion, a process important for both viral and cellular chromosome stability.

Glycyrrhizic acid (GA) is a natural product extracted from licorice root that has biological activities with potential value in the treatment of various diseases and pathologies, including virus infections (8, 14, 20, 30, 31, 42, 43, 47). GA and related metabolites have been shown to inhibit severe acute respiratory syndrome virus entry (6, 18), herpes simplex virus DNA replication (42), and Epstein-Barr virus (EBV) DNA replication and infectivity (30, 31) and to selectively inhibit the proliferation of B lymphocytes latently infected with Kaposi's sarcoma-associated herpesvirus (KSHV) (7, 8, 26). GA can also affect cellular processes, including the attenuation of CpG DNA-stimulated Toll like-receptor (TLR) signaling and the lipopolysaccharide-mediated proinflammatory response (25, 47). GA can also affect transcription by inhibiting the nuclear accumulation of SMAD3 for collagen activation associated with liver fibrosis (35) and can modulate AP-1 transcription factor regulation (19). GA is a triterpenoid saponin glycoside that has molecular components that may mimic steroid hormones, polysaccharides, and nucleic acids (43). For these reasons, the protein targets and molecular pathways affected by GA may be complex and heterogeneous.

KSHV is a human gammaherpesvirus causally associated with Kaposi's sarcoma, pleural effusion lymphoma (PEL), and multicentric Castleman's disease (15, 34, 48). KSHV is thought to establish a long-term infection in B lymphocytes, similar to EBV (54). In latently infected PEL cells, KSHV transcription is restricted to a small subset of viral genes that includes a complex and multicistronic cluster of transcripts that encode LANA (open reading frame 73 [ORF73]), vCyclin (ORF72), and vFLIP (ORF71), as well as the viral microRNAs and kaposin (K12) (2, 11, 40, 45). In primary PEL biopsy specimens, transcripts for adjacent and reverse-oriented genes for vGPCR (ORF74) and K14 are also detected (36). A primary initiation site has been mapped for the major multicistronic transcript encoding LANA, vCyclin, and vFLIP, but the mechanisms that regulate alternative downstream promoter usage and mRNA processing are not completely understood (13, 21, 29, 40). We have found that the chromatin insulator binding protein CTCF and cohesins, which maintain sister chromatin cohesion, co-occupy an ~150-bp region located within first 5′ intron of the multicistronic latency transcript (50). Mutagenesis studies revealed that the CTCF-cohesin binding sites regulate the cell cycle control of latency transcription, as well as restrict lytic transcription in the opposite orientation (23). A similar CTCF-cohesin co-occupancy site was observed at several cellular sites, including the c-*myc* promoter and the Igf2-H19 imprinting locus (50). Cohesins consist of three major components, SMC1, SMC3, and RAD21, that can form ring-like structures thought to link DNA molecules (17). Cohesins function in transcription regulation and sister chromatid cohesion and can be regulated by multiple mechanisms, including proteolysis by separase (55) and lysine acetylation by ESCO proteins (51, 56).

GA inhibits KSHV-infected cell growth through a mechanism that involves the selective suppression of LANA transcription (8). The ORF73 transcript encoding LANA is part of a multicistronic message that can encode ORF72 and ORF71,

* Corresponding author. Mailing address: The Wistar Institute, 3601 Spruce Street, Philadelphia, PA 19104-4268. Phone: (215) 898-9491. Fax: (215) 898-0663. E-mail: lieberman@wistar.org.

▽ Published ahead of print on 31 August 2011.

as well as viral microRNA and K12. However, alternative promoter utilization may also account for the changes in latency transcript formation. Furthermore, K14 and ORF74 initiation in the opposite orientation is thought to be restricted to the lytic phase, but transcripts can be detected in PEL biopsy specimens (36) and are enriched in G_2 phase of the cell cycle in BCBL1 cells (23). KSHV latency transcripts are synthesized by RNA polymerase II (RNAPII), which can be regulated at multiple levels, including initiation, elongation, and mRNA processing. KSHV latency transcription appears to be directed largely through a strong core promoter and initiator element with no obvious upstream enhancer-like factors. Determinants of promoter initiation, transcription orientation, splice site selection, and mRNA processing remain poorly understood. Studies of other viruses and many cellular proteins have revealed that many RNAPII genes are regulated at the level of elongation (12, 37, 41). Several accessory factors bind to the carboxy-terminal domain (CTD) of the RNAPII large subunit to regulate the transition between initiation and elongation, as well as loading of mRNA processing factors that function cotranscriptionally (27, 49). The negative elongation factor (NELF) consists of several protein components that restrict the elongation of RNAPII (5). The positive transcription elongation factor (P-TEFb) consists of a protein kinase that can phosphorylate the CTD on S2 to promote elongation. Transcription initiation is regulated by the general transcription factors, including kinase-containing TFIIH, which phosphorylates the CTD on S5. Cycling between the phospho-S5 and -S2 forms of the CTD is an important regulatory mechanism of RNAPII transcription. The DSIF complex, which consists of the SPT4 and SPT5 proteins, can also promote RNAPII elongation through direct interaction with the phospho-S2 isoform of the CTD (3). Precisely how these factors may regulate RNAPII at the KSHV major latency transcription cluster has not been investigated, nor has the molecular mechanism through which GA selectively inhibits LANA transcription been elucidated. In this study, we explored the mechanism of GA suppression of LANA transcription, and here we provide evidence that GA interacts with components of the cohesin and DSIF complexes to deregulate KSHV latency transcription.

MATERIALS AND METHODS

Cells. The KSHV-positive PEL cell line BCBL1 was cultured at 37°C and 5% CO_2 in RPMI 1640 medium (Gibco BRL) supplemented with 10% fetal bovine serum and penicillin-streptomycin (50 U/ml). Lytic activation of KSHV was induced in BCBL1 cells by the addition of 1 mM sodium butyrate (NaB) plus 20 ng/ml phorbol ester (TPA) for 48 h of incubation. 5,6-Dichloro-1-β-D-ribofuranosylbenzimidazole (DRB; Sigma) was added to BCBL1 cells at 5 or 10 μM for 48 h of incubation, as indicated.

GA treatment. For cell-based assays, dry GA powder (Sigma catalog no. 0531-50G) was dissolved completely in complete RPMI medium at either 2 mM or 4 mM by shaking at 200 rpm at 37°C for 30 min. GA treatment was performed by adding 0.5×10^6 BCBL1 cells per ml of RPMI medium containing dissolved GA and incubating them at 37°C and 5% CO_2 for 48 h (unless otherwise indicated).

Colcemid treatment. BCBL1 cells (2×10^6) were placed into 20 ml of fresh RPMI medium and incubated at 37°C and 5% CO_2 for 24 h prior to treatment with 200 μl of colcemid (Sigma) for 2.5 h to arrest the BCBL1 cells in metaphase. The arrested cells were pelleted by centrifugation at 900 rpm in a tabletop centrifuge and resuspended in 10 ml of 0.075 M KCl for 30 min at 37°C to swell the cells. Cells were then fixed by resuspension in 10 ml of ice-cold methanol-acetic acid (3:1) solution for 10 min twice. Cells were then resuspended with 250 μl of methanol-acetic acid (3:1) solution, dropped onto glass slides from a 12-cm height, and then allowed to air dry overnight. The next day, the glass slides were mounted with 4′,6-diamidino-2-phenylindole (DAPI) and analyzed by microscopy.

Cell cycle analysis. Centrifugal elutriation was used to separate BCBL1 and 293T cells into different cell cycle phases, with flow rates of 15, 18, 21, 24, 27, 30, 34, 38, 42, and 46 ml/min, as described previously (23). Fluorescence-activated cell sorter (FACS) analysis of propidium iodine (PI)-stained, fractionated cells was carried out after each centrifugal elutriation.

Antibodies. Antibodies were obtained from the following sources: IgG, Santa Cruz Biotechnology; KSHV LANA, Advanced Biotechnology; β-actin, Bethyl; CTCF, Bethyl; RAD21, Bethyl; SMC3, Bethyl; SMC1, Bethyl; RNAPII-S5, Abcam; RNAPII-S2, Abcam; NELF-A, Bethyl; SPT5, Bethyl; TFII1, Abcam; H3K4me3, Millipore; H3K9me3, Millipore; H3K36me3, Abcam; 5-methylcytidine, Abcam; MCM3, Abcam; MCM7, Abcam; FBP1, Santa Cruz Biotechnology; ESCO2, Bethyl; PCNA, Santa Cruz Biotechnology.

Quantitative reverse transcriptase PCR (qRT-PCR). Total RNAs were extracted by the use of an RNeasy kit (Qiagen) and then further treated with DNase I (Ambion). A total of 2 μg of the RNA was subjected to a SuperScript II RNase H^- RT (Invitrogen) reaction with 5 μM random decamers (Ambion) according to the manufacturers' protocols. Diluted RT products were analyzed by real-time PCR (ABI Prism 7000 sequence detection system; Applied Biosystems). The primers used in this qRT-PCR assay are available upon request. The level of β-actin in each sample was used as the internal control for each quantitative PCR. A quantitative PCR assay with RNA without reverse transcription was conducted to serve as a negative control for each reaction. Semiquantitative RT-PCR was performed essentially as described previously (23). Starting with 2 μg of RNA, RT products were synthesized as described above, followed by DNase I treatment and purification using a QIAquick PCR purification kit (Qiagen). Equal amounts of RT products were subjected to the semiquantitative RT-PCR assay. Semiquantification of the complete latent transcript (LTc), latent transcript 1 (LT1), latent transcript 2 (LT2), the lytic transcript of ORFK14/74 (LyTc), and the 5′-end intron region of the ORF73/72/71 transcript was conducted relative to β-actin and glyceraldehyde 3-phosphate dehydrogenase (GAPDH). A semiquantitative PCR assay with RNAs without reverse transcription was conducted to serve as a negative control for each reaction. The primers used in this semiquantitative RT-PCR assay are available upon request.

Northern blotting. BCBL1 cells were left untreated or treated with 2 or 4 mM GA for 48 h and subjected to RNA extraction (RNeasy; Qiagen) and on-column DNase I digestion (RNase-Free DNase Set; Qiagen). Northern analysis was conducted as previously described (23). Thirty micrograms of denatured RNA was allowed to migrate on a 1% formaldehyde-agarose gel, transferred to a BrightStar-Plus membrane (Ambion) by the downward capillary transfer method, and cross-linked by UV light. The membrane was prehybridized in digoxigenin (DIG) Easy Hyb buffer and hybridized in ULTRAHyb buffer (Ambion) overnight containing a DIG-labeled DNA probe for LTc (127622 to 127883), LT1 (KSHV 123812 to 124519), LT2 (KSHV 122814 to 123553), LyTc (KSHV 128830 to 130111), or K14 (KSHV 127885 to 128908) transcripts. A β-actin transcript was also quantified as an internal control. The primers used in generating DIG-labeled DNA probes are available upon request.

GA affinity purification. CarboxyLink resin (catalog no. 20266; Pierce/Thermo-Fisher) was washed and resuspended in reaction buffer (0.1 M morpholineethanesulfonic acid, pH 4.7) at 1:1 (vol/vol). Resuspended CarboLink resin was then mixed 1:1 with a solution of 4 mM GA (resuspended in reaction buffer) or with reaction buffer lacking GA (control resin) for 5 min of mixing by end-over-end rotation. An equal volume (~200 μl) of the freshly prepared coupling reagent 1-ethyl-3-(3-dimethylaminopropyl)carbodiimide (EDC; 120 mg/ml) in reaction buffer was added to CarboLink resin samples (with or without GA) and mixed end over end at 25°C for 3 h. Resins were then transferred to a 1-ml chromatography column and allowed to drain by gravity. Columns were then washed with 5 column volumes of 1 M NaCl and allowed to equilibrate for 1 h in 1 M NaCl at 4°C. All remaining procedures were conducted at 4°C. Columns were washed extensively (~10 column volumes) in D buffer (20 mM HEPES, pH 7.9, 20% glycerol, 0.5 mM EDTA, 1 mM dithiothreitol, 1 mM phenylmethylsulfonyl fluoride) containing 100 mM NaCl. One milliliter of BCBL1 cell nuclear extract (~7 mg/ml) (10) previously dialyzed in D buffer containing 100 mM NaCl was incubated with each sealed column with end-over-end mixing for 1 h. Extract was then eluted by gravity, and the column was washed with 5 column volumes of D buffer containing 100 mM NaCl. Proteins were then eluted sequentially with 3×500 ml of D buffer containing 100 mM NaCl, followed by D buffer containing 100 mM NaCl and 2 mM GA. Eluted fractions were assayed by SDS-PAGE and colloidal blue staining. Protein bands deemed to be enriched in the GA resin relative to the control resin were isolated

and subjected to liquid chromatography-tandem mass spectrometry (LC/MS/MS) at the Wistar Institute proteomics facility.

Miscellaneous. Coimmunoprecipitation, chromatin immunoprecipitation (ChIP), Western blotting, and the assay used for determining KSHV DNA copy numbers have been described previously (23). These additional protocols are available upon request.

RESULTS

GA deregulates KSHV latency transcription. GA has been shown to inhibit LANA transcription in latently infected BCLB1 cells (8). To better understand this effect, we assayed the transcription of several viral and cellular genes in BCBL1 cells after treatment with GA (Fig. 1). Consistent with previous reports, we found that transcripts encoding LANA (ORF73) were reduced in BCBL1 cells treated with GA. qRT-PCR with gene-specific primers revealed that the total RNA for ORF73 was reduced ~2- to 3-fold after GA treatment (Fig. 1A). GA also had effects on several other viral genes, including an ~2- to 3-fold reduction in ORF72, which is generated from the same parent transcript as ORF73. In contrast to the reduction in ORF73 and ORF72, GA increased the transcription of the lytic transcript K2 (vIL-6) but did not activate other lytic markers, including ORF50 (Fig. 1A) or the KSHV DNA copy number (Fig. 1E). We also observed that GA treatment reduced cellular c-*myc* RNA but modestly activated TLR7 (Fig. 1A, right panel). These findings indicate that GA treatment alters viral and cellular transcription and that a subset of genes, like ORF73 and c-*myc*, are preferentially inhibited by GA.

RT-PCR with exon-intron junction-specific primers was used to further analyze the effects of GA on specific transcripts generated at the KSHV latency locus (Fig. 1B). The parent multicistronic transcript LTc can be processed into two major species, LT1 (encoding LANA) and LT2 (encoding vCyclin and vFLIP) (4, 40, 45, 46). GA treatment reduced the processed transcripts for LT1 and LT2 to a greater extent than the parent transcript LTc. On the complementary strand, lytic genes for K14 and ORF74 can be expressed as a bicistronic transcript (LyTc) or from a smaller transcript encoding ORF74 only (LyT1). GA treatment reduced both LyTc and LyT2. GA had no detectable effect on cellular actin or GAPDH levels (Fig. 1B). The effects of GA on these transcripts were further analyzed by Northern blotting with probes for LTc (ORF73/ORF72/ORF71), LT1 (ORF73), LT2 (ORF72/71), LyTc (K14/ORF74), and LyT1 (ORF74) (Fig. 1C). Northern blotting revealed a much greater reduction in the LT1 and LT2 transcripts than in the larger LTc transcript. Similarly, the LyT1 transcript was more significantly reduced than the LyTc transcript. Western blot analysis indicated that LANA protein levels were reduced ~3-fold after 48 h of GA treatment, consistent with a decrease in LANA mRNA levels (Fig. 1D). GA treatment did not induce KSHV lytic protein Rta (Fig. 1D), nor did it cause cleavage of cellular PARP1, suggesting that it did not induce caspase-mediated apoptosis at the 48-h time point. Quantitative PCR of viral DNA indicated that GA did not increase the viral DNA copy number, further substantiating that it was not activating the lytic replication cycle (Fig. 1E).

GA affects RNAPII pausing and processing at the CTCF-cohesin binding site. RNA analysis suggested that GA may be affecting RNAPII function in transcription initiation or RNA processing of KSHV latency transcripts. To investigate this possibility, we performed ChIP assays to examine the effect of GA on the binding of several candidate proteins in the latency control region. We first examined the effect of GA on the binding of CTCF and cohesin subunits SMC3 and RAD21 (Fig. 2A). GA treatment caused a modest increase in SMC3 and RAD21 binding but an ~2-fold reduction in CTCF binding, suggesting that it may be affecting the typical interactions between cohesins and CTCF.

To determine whether GA affects RNAPII occupancy or function at the KSHV latency locus, we performed ChIP with antibodies specific for either the phospho-S5 or the phospho-S2 isoform of RNAPII (Fig. 2B). We found that RNAPII-S5, the isoform associated with polymerase pausing, was highly enriched at the CTCF-cohesin binding site (Fig. 2B, top panel). More interestingly, GA treatment completely abrogated this enrichment. RNAPII-S2, the isoform associated with elongation, was enriched throughout the latency transcripts, with peak occupancy near the LTc transcription start site. GA treatment reduced the overall occupancy of the S2 form of RNAPII throughout the latency locus. RNAP II NELF-A and elongation factor SPT5 were also enriched at the CTCF-cohesin binding site, showing a ChIP pattern similar to that of RNAPII-S5. GA treatment led to a loss of NELF-A and SPT5 binding at the CTCF-cohesin binding sites, similar to that observed with RNAPII-S5. TFII-I, a factor that has been implicated in RNAPII initiation and regulation, was also enriched at the CTCF-cohesin site but only after GA treatment. These findings suggest that GA treatment alters the interaction of RNAPII and associated regulatory factors with the KSHV latency control region.

To further explore the effects of GA on the chromatin of the latency control region, we examined several histone modifications by ChIP assay and DNA methylation by methyl-DNA immunoprecipitation (MeDIP) assay (Fig. 2C). As previously reported, histone H3K4me3 was enriched at the CTCF-cohesin binding sites, but this enrichment was reduced only slightly (<2-fold) by GA treatment. The histone H3K9me3 level was low throughout the latency region but was elevated at a distal lytic region, ORF34. GA treatment had little detectable effect on H3K9me3. H3K36me3, a modification associated with RNAPII and mRNA processing, was elevated downstream of ORF73, within ORF71, as well as in K14 and ORF74. GA treatment caused a general reduction in H3K36me3 at all of the sites assayed. The MeDIP assay detected methylcytosine downstream of ORF73 and within ORF74, but these signals were unaffected by GA treatment. These data suggest that GA has only modest effects on histone modifications in the latency control region, with the most notable effect on the reduction of H3K36me3.

The effect of GA on chromatin and RNAPII factors was also examined at several cellular chromosomal sites (Fig. 3). As previously reported, CTCF and cohesins (e.g., SMC3) were highly enriched at the *myc* MINE locus relative to other regions, including *myc* P2, actin, and GAPDH (16) (Fig. 3A). GA caused an ~2-fold reduction in CTCF binding and a modest increase in SMC3 at *myc* MINE, similar to that observed with the KSHV LANA control region. We found that RNAPII-S5, but not RNAPII-S2, was enriched at the *myc* P2 region.

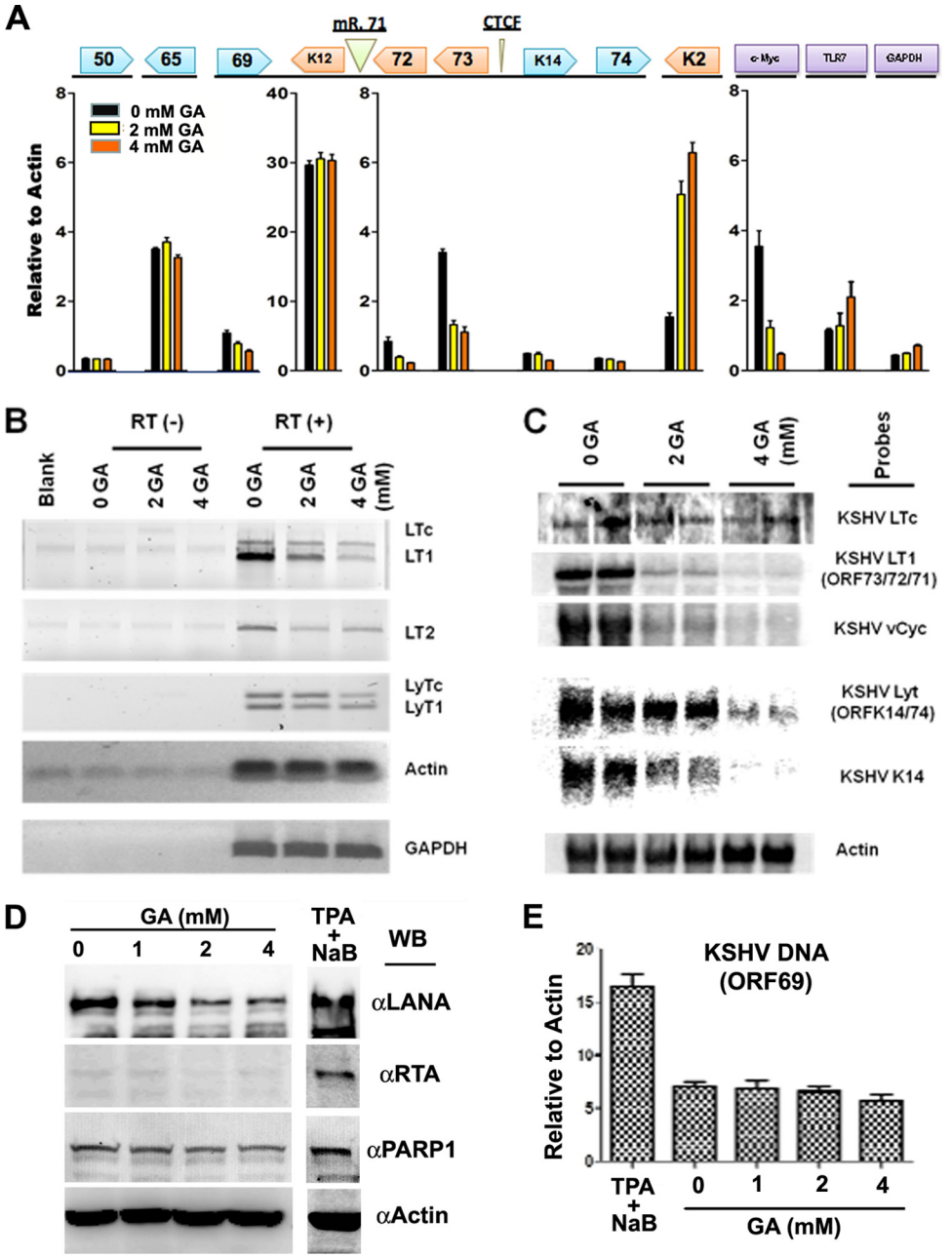

FIG. 1. Effects of GA on KSHV gene transcription in BCLB1 cells. (A) Real-time RT-PCR analysis of KSHV mRNA for ORF50, ORF65, ORF69, ORF72, ORF73, K14, ORF74, and K2 (as indicated above each data set) relative to cellular actin. RNA was isolated from BCBL1 cells left untreated (black) or treated with 2 mM (yellow) or 4 mM (orange) GA. (B) Conventional RT-PCR analysis of KSHV transcripts for LTc, LT1, LT2, LyTc, or LyT1 and cellular transcripts for actin or GAPDH, as indicated. RNA was isolated from BCLB1 cells left untreated or treated with 2 or 4 mM GA, as indicated. The no-RT (−) controls used are shown on the right. (C) Northern blot analysis of untreated (0 mM) or GA-treated (2 mM or 4 mM) BCLB1 cell RNA, as indicated above each lane, shown as experimental duplicates. A Northern blot of RNA was probed for KSHV LTc, LT1, vCyclin (ORF72), Lyt (K14//ORF74), K14, or cellular β-actin. (D) Western blotting (WB) of BCBL1 cells treated with 0, 1, 2, or 4 mM GA or with the lytic KSHV activation-inducing agents NaB (1 mM) and TPA (20 ng/ml) and assay with antibodies for LANA, Rta, PARP1, or actin. (E) Real-time PCR of the total intracellular KSHV genome DNA copy number relative to actin after treatment with NaB (1 mM) plus TPA (20 ng/ml) or 0, 1, 2, or 4 mM GA.

NELF-A and, to a lesser extent, SPT5 colocalized with RNAPII-S2 in the *myc* P2 region. GA treatment caused a substantial loss of RNAPII-S5, NELF-A, and SPT5 in the *myc* P2 region. High levels of RNAPII-S5 and SPT5 were observed in the actin gene. GA did not affect RNAPII-S5 binding but did reduce SPT5 binding at the highest doses. As reported, histone H3K4me3 was enriched at the CTCF-cohesin binding site (Fig. 3B). H3K9me3, H3K36me3, and MeDIP were elevated at the actin locus, but GA had little effect on these modifications at these sites.

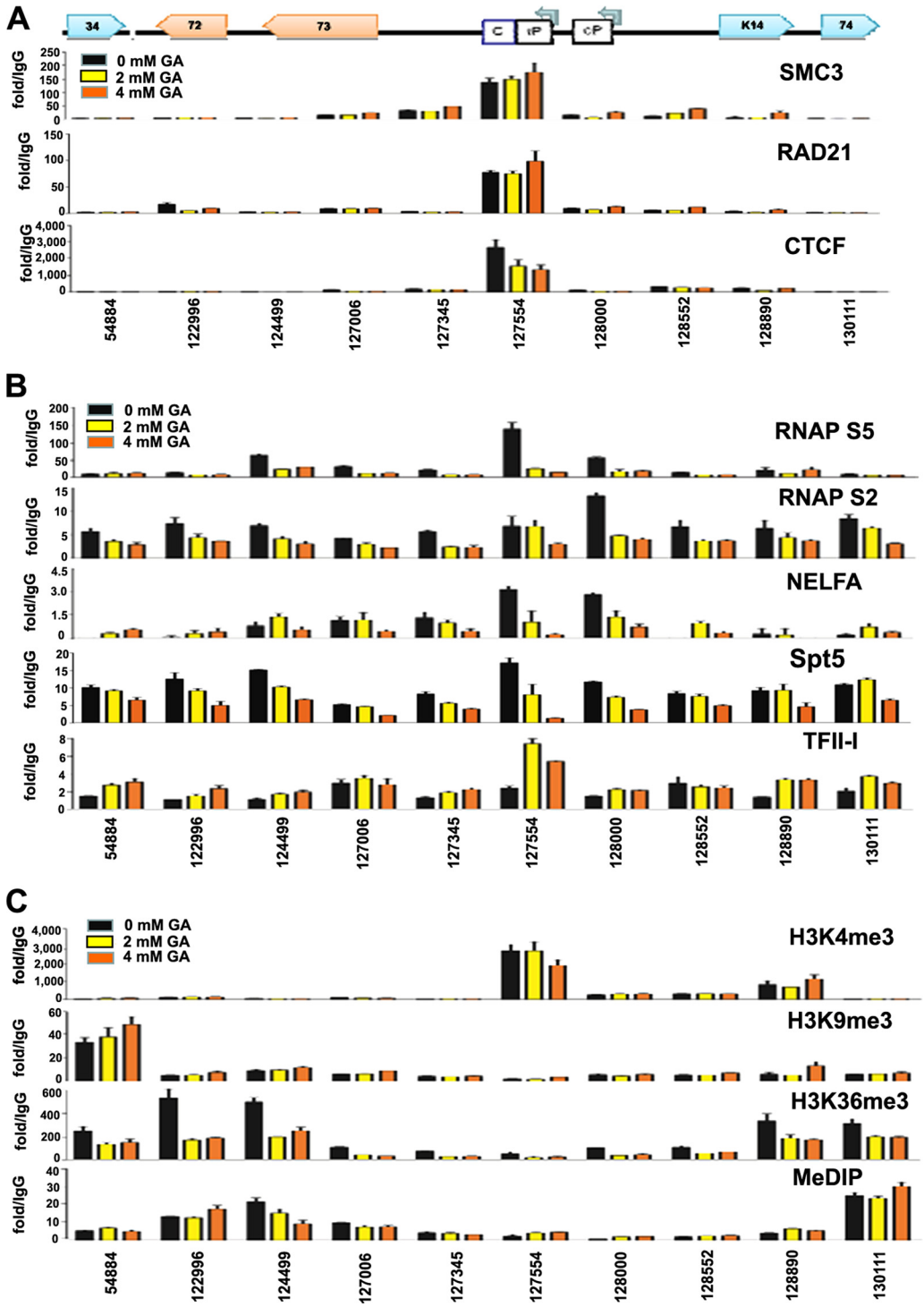

FIG. 2. Effect of GA on KSHV latency control region chromatin regulators. ChIP and MeDIP assays were performed with BCBL1 cells left untreated (black) or treated with 2 mM (yellow) or 4 mM (orange) GA. ChIP or MeDIP DNA was quantified by real-time PCR with primers for the regions indicated above each set, including ORF34, ORF72, ORF73, the CTCF-cohesin binding site (C), the inducible promoter (iP), the constitutive promoter (cP), K14, and ORF74. (A) ChIP assays with antibodies to SMC3 and CTCF. (B) ChIP assays with antibodies to RNAPII-S5, RNAPII-S2, NELF-A, SPT5, and TFIII. (C) ChIP assays with antibodies to histone H3K4me3, H3K9me3, and H3K36me3 and MeDIP assay, as indicated.

GA alters RNAPII and cohesin interactions. The effect of GA on RNAPII and cohesins was further examined by IP-Western blot analysis (Fig. 4). Extracts from untreated or GA treated BCBL1 cells were first assayed by IP with an antibody that recognizes all phospho isoforms of RNAPII (Fig. 4A). We assayed interactions of RNAPII with SPT5, SMC1, SMC3, and CTCF by Western blotting. We found a weak interaction between RNAPII and SPT5, SMC1, and SMC3 but no detectable

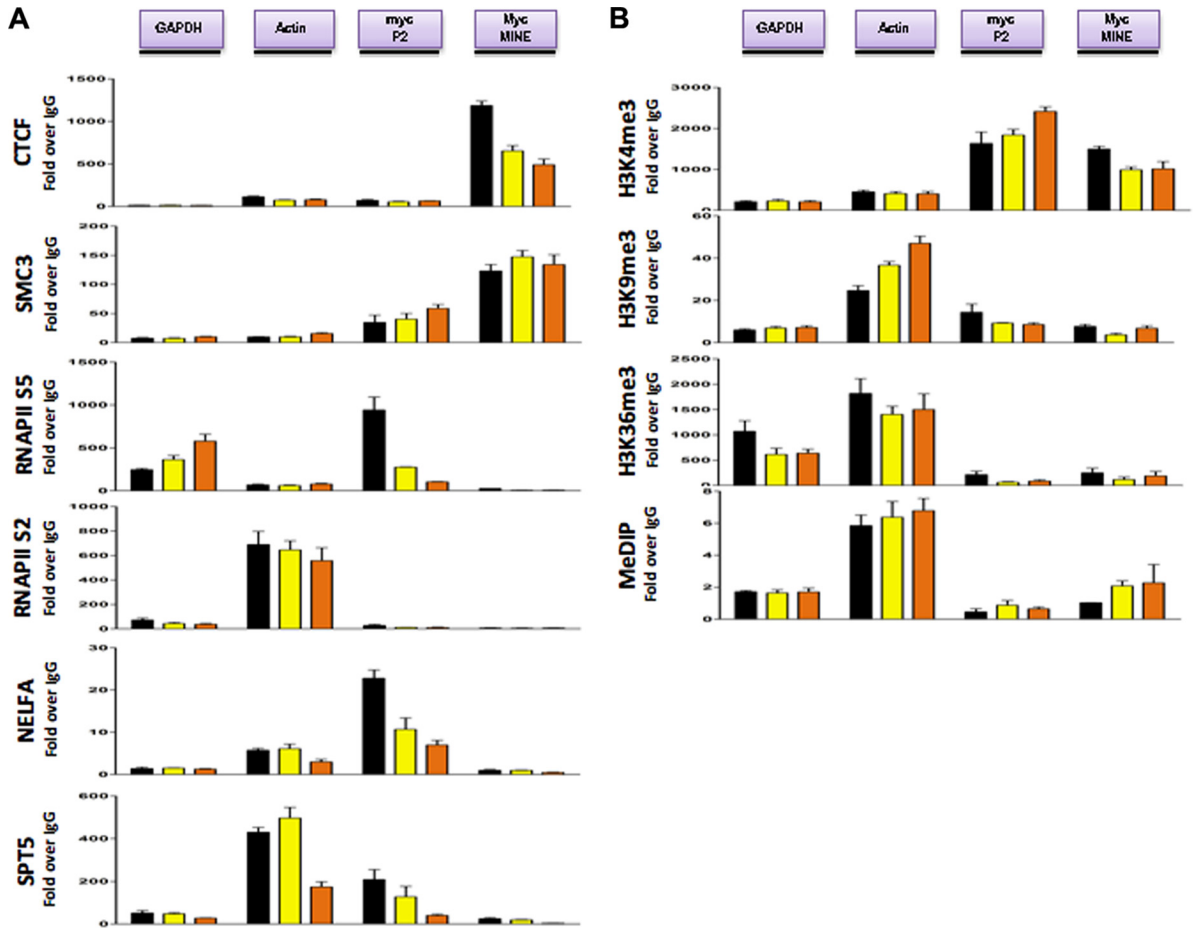

FIG. 3. Effect of GA on cellular gene chromatin regulators. BCBL1 cells were treated with 0 (black), 2 (yellow), or 4 (orange) mM GA, as indicated. ChIP assays examined GAPDH, actin, c-*myc* P2, and the c-*myc* MINE regulatory region, as indicated. (A) ChIP assays for CTCF, SMC3, RNAPII-S5, RNAPII-S2, NELF-A, and SPT5. (B) ChIP assays for H3K4me3, H3K9me3, H3K39me3, and MeDIP DNA, as indicated.

interaction with CTCF. GA treatment partially inhibited the interactions between RNAPII and SPT5, SMC1, and SMC3 but only at the highest concentration of GA (4 mM). Western blotting with antibody specific for the RNAPII-S2 or -S5 isoform revealed no major loss of phosphorylation but suggested that slower-migrating isoforms of S5 were reduced at 4 mM GA. Since SPT5 is known to preferentially bind RNAPII-S5, we next assayed SPT5-specific immunoprecipitates (Fig. 4B). As expected, RNAPII-S5 preferentially associated with SPT5 in the absence of GA. Interestingly, GA treatment increased the percentage of RNAPII-S2 that coimmunoprecipitates with SPT5 (Fig. 4B, middle right panel). This suggests that GA may alter RNAPII isoform-specific interactions with its accessory factors. We next examined the immunoprecipitates of cohesin subunit SMC3 (Fig. 4C). SMC3 immunoprecipitates showed a weak interaction with SPT5 and CTCF, which was reduced after treatment with high levels of GA (4 mM). SMC3 IP revealed a robust interaction with cohesin subunit RAD21, which was substantially reduced after GA treatment. In contrast, SMC1 remained strongly bound to SMC3 after GA treatment. SMC3 interactions with RAD21 can be regulated by SMC3 lysine acetylation (56). We therefore assayed SMC3 immunoprecipitates with antibody to acetyllysine (acK). We found a strong acK band that comigrated with the SMC3 polypeptide. GA treatment caused a reduction in this acK signal. The levels of SMC3 in SMC3 immunoprecipitates were similar in untreated and treated cells. These findings suggest that GA can affect cohesin interactions, potentially by the disruption of RAD21 binding to SMC1-SMC3 and the loss of acetylated SMC3.

GA affinity purification of cellular proteins. To determine whether GA physically interacts with any of the candidate proteins that regulate latency transcription, we developed a GA affinity purification method (Fig. 5A and B). GA was covalently coupled to a solid Sepharose support using Carboxy-Link resin (Pierce) and the cross-linking agent EDC (Fig. 5B). Nuclear extracts from BCBL1 cells were incubated with either GA-coupled resin or mock-treated resin, washed extensively, and then eluted with 4 mM GA (Fig. 5C). Proteins isolated by this method were subjected to SDS-PAGE and colloidal blue staining. Proteins enriched in the GA affinity resin were subjected to LC/MS/MS for identification. Several polypeptides were identified and validated by Western blotting, including DNA replicative helicase subunits MCM3 and -7, FUSE binding protein 1 (FBP1) (9, 39), SMC3, SPT5, and TFII-I. Several additional proteins were identified by LC/MS/MS but were not investigated further or

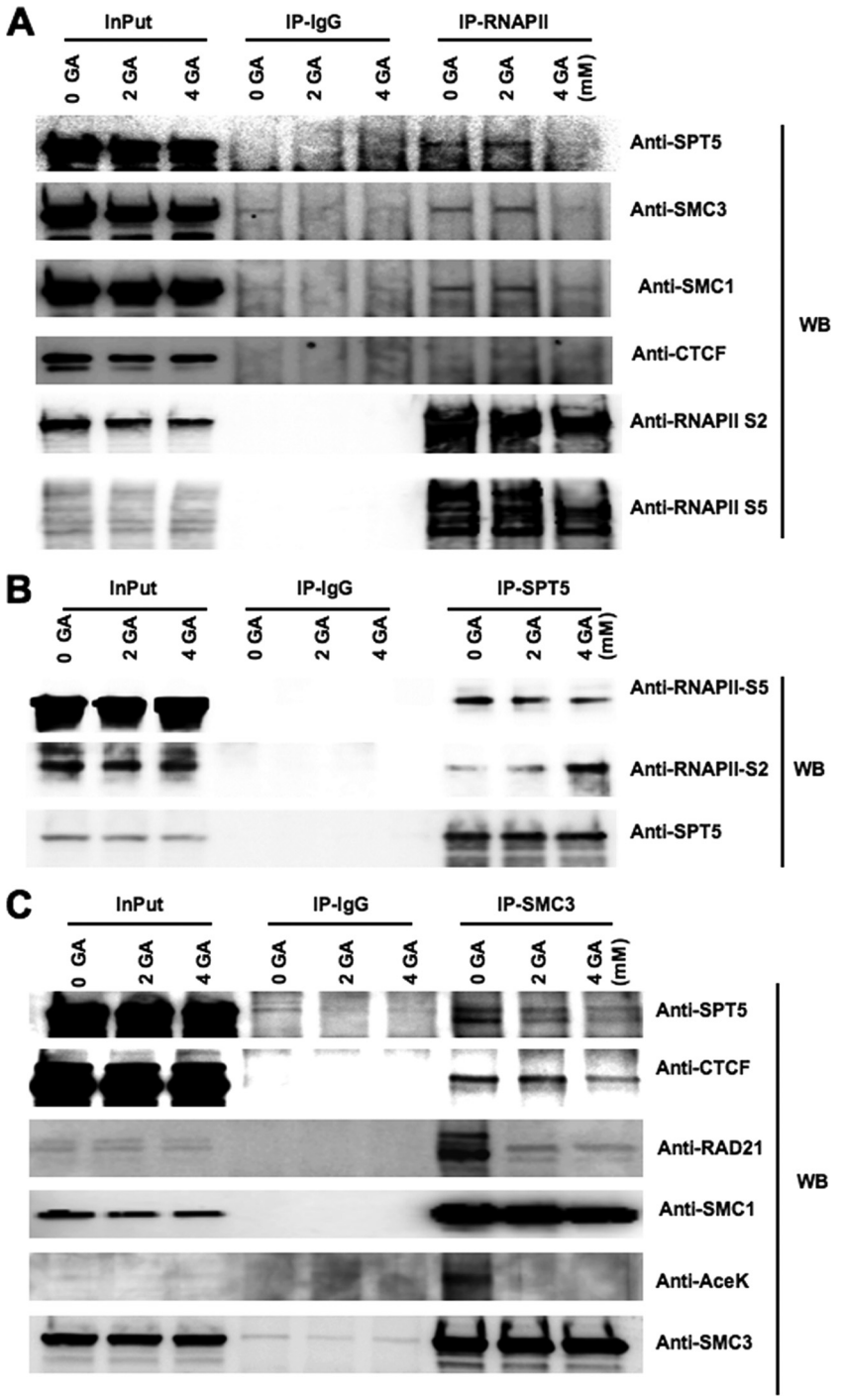

FIG. 4. Effect of GA on RNAPII, SMC3, and SPT5 protein interactions. (A) BCBL1 cells left untreated or treated with 2 or 4 mM GA were subjected to IP with antibody to RNAPII or control IgG and assayed by Western blotting (WB) with antibodies to SPT5, SMC3, SMC1, CTCF, RNAPII-S2, and RNAPII-S5. (B) BCBL1 cells were treated as described for panel A, subjected to IP with antibody to SPT5, and then assayed by Western blotting with antibodies to RNAPII-S5, RNAPII-S2, and SPT5. (C) BCBL1 cells were treated as described for panel A, subjected to IP with antibody to SMC3, and then assayed by Western blotting with antibodies to SPT5, CTCF, RAD21, SMC1, acetyl-lysine, and SMC3.

validated by Western blotting. Neither LC/MS/MS nor Western blotting revealed any interaction of GA with RAD21, the cohesin acetylase ESCO2, RNAPII (S5), CTCF, PCNA, or SMC1. These findings indicate that GA can interact directly or indirectly with a subset of cellular proteins that have implicated functions at the latency control region and the *myc* promoter. In addition, these findings suggest that GA can bind to SMC3 and SPT5 without corecruitment of their partner proteins.

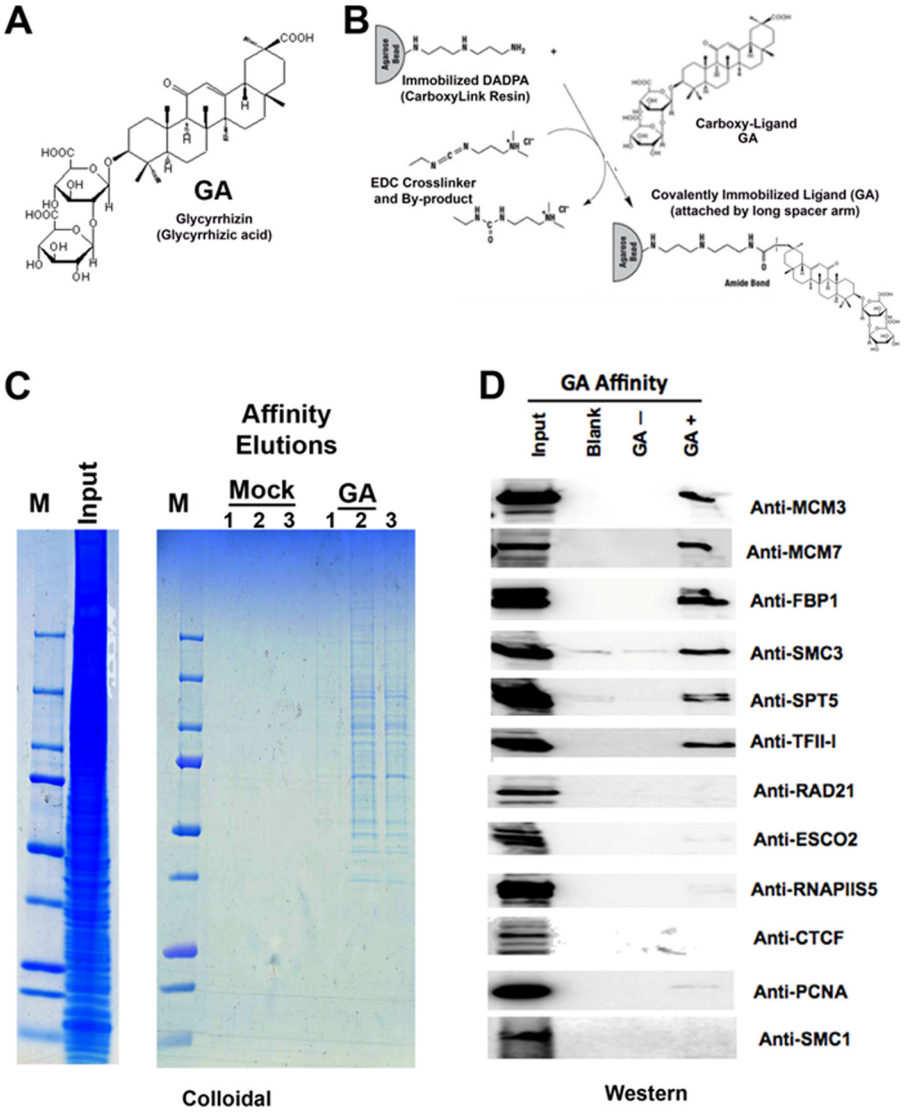

FIG. 5. Identification of GA affinity-purified cellular proteins. (A) Fisher projection structure of GA. (B) Strategy for immobilization of GA on CarboxyLink resin using the cross-linker EDC. (C) Colloidal staining, after SDS-PAGE analysis, of proteins bound to and eluted from GA affinity resin or mock affinity resin after elution with 1 mM GA. Three sequential one-column-volume elutions are shown in lanes 1 to 3, respectively. (D) Western blot analysis for candidate GA affinity-purified proteins identified by LC/MS/MS. Input proteins and mock affinity (GA−) resin- and GA affinity (GA+) resin-purified proteins (as indicated above) were assayed with antibodies for MCM3, MCM7, FPB1, SMC3, SPT5, TFII-I, RAD21, ESCO2, RNA Pol II-S5, CTCF, PCNA, and SMC1, as indicated to the right of each blot.

Defective sister chromatid cohesin in GA-treated BCBL1 metaphase spreads. Since GA affected cohesin interactions, we assayed the effect of GA on the well-established function of cohesins in sister chromatid attachment (Fig. 6). BCBL1 cells were treated with 0, 2, or 4 mM GA and then assayed for cell cycle profile by FACS analysis of PI staining (Fig. 6A). GA treatment caused a general depletion of cells in G_2/M, suggesting that GA causes cell cycle defects. To explore whether GA affects metaphase chromosome organization, we examined metaphase spreads from BCBL1 cells treated with 1 mM GA for 24 h, which allowed more cells to enter G_2/M than did the higher concentrations typically used in functional cell-based assays. BCLB1 cells were arrested in metaphase with colcemid, stained with DAPI, and then assayed visually by microscopy (Fig. 6B). We noted that treatment with 1 mM GA for 24 h induced a phenotype consistent with loss of sister chromatid cohesion. The separated sister chromatids were counted manually, and their number was found to be significantly increased in GA-treated cells ($P < 0.0001$). These findings suggest that GA inhibits sister chromatid cohesion.

Inhibitor of RNAPII elongation blocks K12 transcription and induces KSHV lytic gene activation. To further explore the potential mechanism of RNAPII regulation by GA, we examined the effects of a classic RNAPII inhibitor, DRB, on KSHV gene expression in latently infected BCBL1 cells (Fig. 7). DRB is known to inhibit RNAPII transcription elongation by interfering with the functions of DSIF (DRB sensitivity-inducing factor) and P-TEFb, which regulate RNAPII pausing

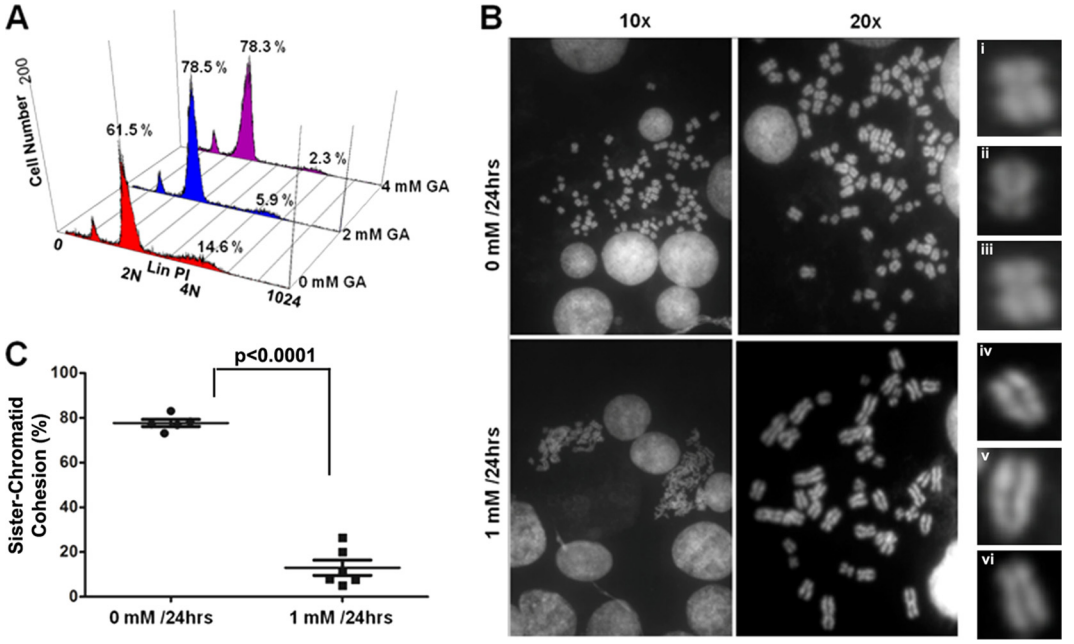

FIG. 6. Effect of GA on sister chromatid cohesion. (A) Cell cycle profile as measured by FACS analysis of PI-stained cells after no treatment or treatment with 2 or 4 mM GA. (B) Metaphase spreads of BCBL1 cells treated with 0 (top) or 1 mM (bottom) GA at ×10 or ×20 magnification. Chromosomes were stained with DAPI. (C) Quantification of separated sister chromatids.

and elongation (37, 38, 52). BCBL1 cells were treated with 5 or 10 μM DRB for 48 h and then assayed by qRT-PCR for changes in KSHV gene expression (Fig. 7). In contrast to GA treatment, we found that DRB treatment induced KSHV lytic gene expression, with an ~2- to 3-fold increase in ORF50 and ORF69 mRNA levels. DRB had only a small stimulating effect on ORF73 and ORF72 mRNA levels but inhibited K12 mRNA ~2- to 3-fold. These results indicate that DRB has an effect on KSHV gene expression that is very different from that of GA and suggest that GA alters RNAPII regulation through a mechanism distinct from that of DRB.

DISCUSSION

In this work, we investigated the mechanisms through which GA selectively deregulates KSHV latency transcription. We confirmed that GA treatment reduces the expression of LANA mRNA and protein (Fig. 1). GA treatment caused a reduction in several transcripts from the latency control region, including the LT1 transcript encoding LANA and the LyT1 transcript encoding ORF74. GA also affected the transcription of the cellular c-*myc* gene (Fig. 1B), suggesting that it is subject to regulation similar to that of KSHV LANA. ChIP assays re-

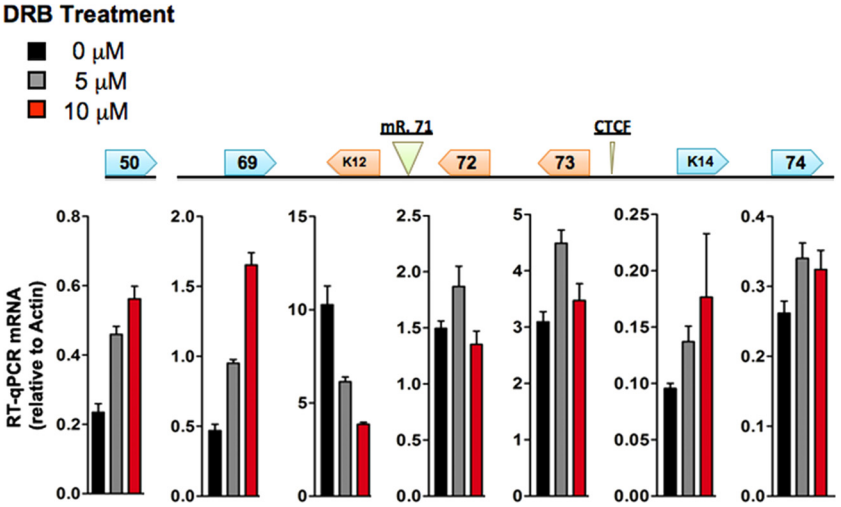

FIG. 7. The RNAPII inhibitor DRB does not inhibit ORF73 expression and induces KSHV lytic cycle gene expression. BCBL1 cells were treated with 0, 5, or 10 μM DRB for 48 h and then assayed for mRNA expression by qRT-PCR using primers specific for ORF50, ORF69, K12, ORF72, ORF73, K14, and ORF74, as indicated. qRT-PCR was normalized to cellular actin.

vealed that RNAPII-S5 and elongation factors NELF-A and SPT5 accumulate at or adjacent to the CTCF-cohesin binding sites in both KSHV LANA and cellular c-*myc*. Treatment with GA eliminated RNAPII-S5, NELF-A, and SPT5 occupancy at these sites (Fig. 2B, and 3A). GA also reduced the enrichment of RNAPII-S2 at the sites of initiation and elongation throughout the KSHV latency transcripts (Fig. 2). Coimmunoprecipitation experiments indicated that GA disrupted interactions between SMC3 and RAD21, as well as reduced the lysine acetylation associated with SMC3 (Fig. 4). GA affinity purification identified both SMC3 and SPT5 as candidate GA-interacting proteins (Fig. 5). GA treatment reduced sister chromatid cohesin of cellular chromosomes, suggesting that it has a global effect on cohesin function (Fig. 6). Taking these findings together, we propose that GA affects components of the cohesin complex that are important for RNAPII pausing and RNA processing. Disruption of these interactions by GA could account for the failure to generate transcripts that are regulated by intragenic CTCF-cohesin bindings sites, like that observed in LANA and c-*myc*.

Mechanism of GA action. We have used chemical affinity chromatography coupled with LC-MS-MS to identify potential protein targets of GA. Our studies focused on cellular proteins enriched in nuclear extracts from BCBL1 cells. We identified several candidates, including SPT5, SMC3, MCM, TFII-I, and FBP1. SPT5 is a component of DSIF and is important for RNAPII pausing and elongation (41). SMC3 is a core component of cohesins (17). TFII-I is involved in RNAPII initiation (44). FBP1 has been implicated in the regulation of c-*myc* transcription (28), as well as HCV infection (57), and could account for some of the anticancer and antiviral activities attributed to GA. It is not clear which, if any, of these proteins are direct binding partners of GA. Our data suggest that GA can interact with a form of SMC3 that is uncoupled from SMC1 and RAD21 (Fig. 5) and suppress lysine acetylation of SMC3 (Fig. 4). GA treatment also disrupted the cohesin function in sister chromatid cohesion (Fig. 6). These findings suggest that GA can interact with and modulate cohesin subunits, as well as interact with components of the RNAPII pausing machinery (e.g., SPT5).

GA has also been implicated in interactions with several other proteins, including the high-mobility group B (HMGB) protein (33). HMGB is a chromatin-associated protein that can affect many processes, including RNAPII functions. However, GA was found to interact with a cytoplasmic and extracellular form of HMGB involved in inflammatory cytokine signaling (33, 58). We also identified HMGB as a minor species in our LC/MS/MS analysis (data not shown). Our affinity purification focused on nuclear proteins, and this may explain why we did not identify HMGB among the more abundant interacting nuclear proteins. Interestingly, we observed that GA could induce KSHV K2 (vIL-6) and cellular TLR7 (Fig. 4), consistent with GA's affecting cytokine production and HMGB cytokine signaling (25, 47). However, we have not explored whether GA interaction with extracellular HMGB and the activation of inflammatory cytokines are linked to GA regulation of RNAPII at the KSHV latency locus.

Implications for transcription control by CTCF-cohesin. Our findings suggest that the KSHV latency control region, as well as the c-*myc* gene, is regulated by multiple factors that control RNAPII programming. These include the initiator element at the transcriptional start site and the CTCF-cohesin cluster within the first intron. ChIP analyses suggest that the CTCF-cohesin sites play a role in regulating RNAPII pausing. RNAPII pausing has been implicated in the control of many cellular genes and is likely to be important for the proper programming of RNAPII in the generation of appropriately spliced and processed mRNAs (37). With a few exceptions, the mechanisms that determine sites of RNAPII pausing are not well defined. In the HIV genome, the TAR RNA structure restricts RNAPII progression, and HIV TAT protein recruitment of P-TEFb relieves this block to elongation (24). Genome-wide studies have found that RNAPII pauses within the first 100 nucleotides of the transcription start sites of many actively transcribed genes (37). In one study, RNAPII pause sites were found to correlate with intragenic CTCF-cohesin binding sites (53). We found that RNAPII-S5 was enriched at the CTCF-cohesin binding site found within the first intron of the KSHV latency transcript, as well as the cellular c-*myc* gene. We propose that these CTCF-cohesin binding sites function as a programmed pause site for RNAPII and that RNAPII pausing facilitates the assembly of RNAPII accessory factors essential for mRNA splicing and maturation. This is consistent with recent studies showing that cohesins regulate RNAPII activity (1, 22) and that alternative RNA splicing can be regulated by chromatin structure and histone modifications (32).

How CTCF, cohesins, and RNAPII accessory factors interact and regulate mRNA maturation remains unknown. Our IP data suggest that weak interactions exist between SPT5 and SMC3, and this may facilitate the assembly of additional mRNA processing factors with RNAPII. Our data further suggest that small molecules like GA may be helpful in elucidating the mechanisms linking RNA pausing with mRNA processing. GA affinity purification recovered several candidate proteins, like SMC3 and SPT5, which could account for its effect on RNAPII pausing at CTCF-cohesin binding sites. While GA can also bind to multiple additional proteins, like HMGB, and affect various cellular pathways, including TLR4 signaling, our findings indicate that RNAPII programming and RNA processing are important functional targets of GA. Our data also suggest that GA functions through a different mechanism than DRB, since these compounds have very different effects on KSHV gene regulation (Fig. 7). While GA and DRB can both interact with DSIF components, GA does not appear to block P-TEFb function and RNAPII-S2 phosphorylation (Fig. 4). Thus, studies of GA may help to identify new regulatory steps in RNAPII processing of mRNA, as well as identify more selective inhibitors of KSHV latency and viral gene expression.

ACKNOWLEDGMENTS

We acknowledge the Wistar Institute core facilities for flow cytometry, microscopy, proteomics, and genomics.

This work was funded by the Wistar Institute Cancer Center grant (P30 CA10815), NIH grant RO1 CA117830 to P.M.L., and a postdoctoral fellowship to H.K. from the Wistar Institute Cancer Center training grant (T32: CA09171-31).

REFERENCES

1. **Bose, T., and J. L. Gerton.** 2010. Cohesinopathies, gene expression, and chromatin organization. J. Cell Biol. **189:**201–210.
2. **Cai, X., and B. R. Cullen.** 2006. Transcriptional origin of Kaposi's sarcoma-associated herpesvirus microRNAs. J. Virol. **80:**2234–2242.

3. **Chiba, K., J. Yamamoto, Y. Yamaguchi, and H. Handa.** 2010. Promoter-proximal pausing and its release: molecular mechanisms and physiological functions. Exp. Cell Res. **316:**2723–2730.
4. **Chiou, C. J., et al.** 2002. Patterns of gene expression and a transactivation function exhibited by the vGCR (ORF74) chemokine receptor protein of Kaposi's sarcoma-associated herpesvirus. J. Virol. **76:**3421–3439.
5. **Choo, S., S. Schroeder, and M. Ott.** 2010. CYCLINg through transcription: posttranslational modifications of P-TEFb regulate transcription elongation. Cell Cycle **9:**1697–1705.
6. **Cinatl, J., et al.** 2003. Glycyrrhizin, an active component of liquorice roots, and replication of SARS-associated coronavirus. Lancet **361:**2045–2046.
7. **Cohen, J. I.** 2005. Licking latency with licorice. J. Clin. Invest. **115:**591–593.
8. **Curreli, F., A. E. Friedman-Kien, and O. Flore.** 2005. Glycyrrhizic acid alters Kaposi sarcoma-associated herpesvirus latency, triggering p53-mediated apoptosis in transformed B lymphocytes. J. Clin. Invest. **115:**642–652.
9. **Davis-Smyth, T., R. C. Duncan, T. Zheng, G. Michelotti, and D. Levens.** 1996. The far upstream element-binding proteins comprise an ancient family of single-strand DNA-binding transactivators. J. Biol. Chem. **271:**31679–31687.
10. **Dignam, J. D., R. M. Lebovitz, and R. G. Roeder.** 1983. Accurate transcription initiation by RNA polymerase II in a soluble extract from isolated mammalian nuclei. Nucleic Acids Res. **11:**1475–1489.
11. **Dittmer, D., et al.** 1998. A cluster of latently expressed genes in Kaposi's sarcoma-associated herpesvirus. J. Virol. **72:**8309–8315.
12. **Egloff, S., and S. Murphy.** 2008. Cracking the RNA polymerase II CTD code. Trends Genet. **24:**280–288.
13. **Fakhari, F. D., and D. P. Dittmer.** 2002. Charting latency transcripts in Kaposi's sarcoma-associated herpesvirus by whole-genome real-time quantitative PCR. J. Virol. **76:**6213–6223.
14. **Fiore, C., et al.** 2008. Antiviral effects of Glycyrrhiza species. Phytother. Res. **22:**141–148.
15. **Ganem, D.** 2006. KSHV infection and the pathogenesis of Kaposi's sarcoma. Annu. Rev. Pathol. **1:**273–296.
16. **Gombert, W. M., et al.** 2003. The c-*myc* insulator element and matrix attachment regions define the c-*myc* chromosomal domain. Mol. Cell. Biol. **23:**9338–9348.
17. **Hirano, T.** 2006. At the heart of the chromosome: SMC proteins in action. Nat. Rev. Mol. Cell Biol. **7:**311–322.
18. **Hoever, G., et al.** 2005. Antiviral activity of glycyrrhizic acid derivatives against SARS-coronavirus. J. Med. Chem. **48:**1256–1259.
19. **Hsiang, C. Y., I. L. Lai, D. C. Chao, and T. Y. Ho.** 2002. Differential regulation of activator protein 1 activity by glycyrrhizin. Life Sci. **70:**1643–1656.
20. **Ito, M., et al.** 1988. Mechanism of inhibitory effect of glycyrrhizin on replication of human immunodeficiency virus (HIV). Antiviral Res. **10:**289–298.
21. **Jeong, J., J. Papin, and D. Dittmer.** 2001. Differential regulation of the overlapping Kaposi's sarcoma-associated herpesvirus vGCR (orf74) and LANA (orf73) promoters. J. Virol. **75:**1798–1807.
22. **Kagey, M. H., et al.** 2010. Mediator and cohesin connect gene expression and chromatin architecture. Nature **467:**430–435.
23. **Kang, H., and P. M. Lieberman.** 2009. Cell cycle control of Kaposi's sarcoma-associated herpesvirus latency transcription by CTCF-cohesin interactions. J. Virol. **83:**6199–6210.
24. **Karn, J.** 2011. The molecular biology of HIV latency: breaking and restoring the Tat-dependent transcriptional circuit. Curr. Opin. HIV AIDS **6:**4–11.
25. **Kim, Y. W., et al.** 2008. Anti-inflammatory effects of liquiritigenin as a consequence of the inhibition of NF-kappaB-dependent iNOS and proinflammatory cytokines production. Br. J. Pharmacol. **154:**165–173.
26. **Klass, C. M., and M. K. Offermann.** 2005. Targeting human herpesvirus-8 for treatment of Kaposi's sarcoma and primary effusion lymphoma. Curr. Opin. Oncol. **17:**447–455.
27. **Lenasi, T., and M. Barboric.** 2010. P-TEFb stimulates transcription elongation and pre-mRNA splicing through multilateral mechanisms. RNA Biol. **7:**145–150.
28. **Levens, D.** 2008. How the c-myc promoter works and why it sometimes does not. J. Natl. Cancer Inst. Monogr. **2008:**41–43.
29. **Li, H., T. Komatsu, B. J. Dezube, and K. M. Kaye.** 2002. The Kaposi's sarcoma-associated herpesvirus K12 transcript from a primary effusion lymphoma contains complex repeat elements, is spliced, and initiates from a novel promoter. J. Virol. **76:**11880–11888.
30. **Lin, J. C.** 2003. Mechanism of action of glycyrrhizic acid in inhibition of Epstein-Barr virus replication in vitro. Antiviral Res. **59:**41–47.
31. **Lin, J. C., et al.** 2008. Inhibitory effects of some derivatives of glycyrrhizic acid against Epstein-Barr virus infection: structure-activity relationships. Antiviral Res. **79:**6–11.
32. **Luco, R. F., et al.** 2010. Regulation of alternative splicing by histone modifications. Science **327:**996–1000.
33. **Mollica, L., et al.** 2007. Glycyrrhizin binds to high-mobility group box 1 protein and inhibits its cytokine activities. Chem. Biol. **14:**431–441.
34. **Moore, P. S., and Y. Chang.** 2003. Kaposi's sarcoma-associated herpesvirus immunoevasion and tumorigenesis: two sides of the same coin? Annu. Rev. Microbiol. **57:**609–639.
35. **Moro, T., et al.** 2008. Glycyrrhizin and its metabolite inhibit Smad3-mediated type I collagen gene transcription and suppress experimental murine liver fibrosis. Life Sci. **83:**531–539.
36. **Nador, R. G., et al.** 2001. Expression of Kaposi's sarcoma-associated herpesvirus G protein-coupled receptor monocistronic and bicistronic transcripts in primary effusion lymphomas. Virology **287:**62–70.
37. **Nechaev, S., and K. Adelman.** 2011. Pol II waiting in the starting gates: regulating the transition from transcription initiation into productive elongation. Biochim. Biophys. Acta **1809:**34–45.
38. **Nechaev, S., et al.** 2010. Global analysis of short RNAs reveals widespread promoter-proximal stalling and arrest of Pol II in Drosophila. Science **327:**335–338.
39. **Olanich, M. E., B. L. Moss, D. Piwnica-Worms, R. R. Townsend, and J. D. Weber.** 2011. Identification of FUSE-binding protein 1 as a regulatory mRNA-binding protein that represses nucleophosmin translation. Oncogene **30:**77–86.
40. **Pearce, M., S. Matsumura, and A. C. Wilson.** 2005. Transcripts encoding K12, v-FLIP, v-cyclin, and the microRNA cluster of Kaposi's sarcoma-associated herpesvirus originate from a common promoter. J. Virol. **79:**14457–14464.
41. **Peterlin, B. M., and D. H. Price.** 2006. Controlling the elongation phase of transcription with P-TEFb. Mol. Cell **23:**297–305.
42. **Pompei, R., O. Flore, M. A. Marccialis, A. Pani, and B. Loddo.** 1979. Glycyrrhizic acid inhibits virus growth and inactivates virus particles. Nature **281:**689–690.
43. **Pompei, R., S. Laconi, and A. Ingianni.** 2009. Antiviral properties of glycyrrhizic acid and its semisynthetic derivatives. Mini Rev. Med. Chem. **9:**996–1001.
44. **Roy, A. L., S. Malik, M. Meisterernst, and R. G. Roeder.** 1993. An alternative pathway for transcription initiation involving TFII-I. Nature **365:**355–359.
45. **Sarid, R., O. Flore, R. A. Bohenzky, Y. Chang, and P. S. Moore.** 1998. Transcription mapping of the Kaposi's sarcoma-associated herpesvirus (human herpesvirus 8) genome in a body cavity-based lymphoma cell line (BC-1). J. Virol. **72:**1005–1012.
46. **Sarid, R., J. S. Wiezorek, P. S. Moore, and Y. Chang.** 1999. Characterization and cell cycle regulation of the major Kaposi's sarcoma-associated herpesvirus (human herpesvirus 8) latent genes and their promoter. J. Virol. **73:**1438–1446.
47. **Schröfelbauer, B., et al.** 2009. Glycyrrhizin, the main active compound in liquorice, attenuates pro-inflammatory responses by interfering with membrane-dependent receptor signalling. Biochem. J. **421:**473–482.
48. **Schulz, T. F.** 2006. The pleiotropic effects of Kaposi's sarcoma herpesvirus. J. Pathol. **208:**187–198.
49. **Selth, L. A., S. Sigurdsson, and J. Q. Svejstrup.** 2010. Transcript elongation by RNA polymerase II. Annu. Rev. Biochem. **79:**271–293.
50. **Stedman, W., et al.** 2008. Cohesins localize with CTCF at the KSHV latency control region and at cellular c-myc and H19/Igf2 insulators. EMBO J. **27:**654–666.
51. **Terret, M. E., R. Sherwood, S. Rahman, J. Qin, and P. V. Jallepalli.** 2009. Cohesin acetylation speeds the replication fork. Nature **462:**231–234.
52. **Wada, T., et al.** 1998. DSIF, a novel transcription elongation factor that regulates RNA polymerase II processivity, is composed of human Spt4 and Spt5 homologs. Genes Dev. **12:**343–356.
53. **Wada, Y., et al.** 2009. A wave of nascent transcription on activated human genes. Proc. Natl. Acad. Sci. U. S. A. **106:**18357–18361.
54. **Wen, K. W., and B. Damania.** 2010. Kaposi sarcoma-associated herpesvirus (KSHV): molecular biology and oncogenesis. Cancer Lett. **289:**140–150.
55. **Wirth, K. G., et al.** 2006. Separase: a universal trigger for sister chromatid disjunction but not chromosome cycle progression. J. Cell Biol. **172:**847–860.
56. **Zhang, J., et al.** 2008. Acetylation of Smc3 by EcoI is required for S phase sister chromatid cohesion in both human and yeast. Mol. Cell **31:**143–151.
57. **Zhang, Z., D. Harris, and V. N. Pandey.** 2008. The FUSE binding protein is a cellular factor required for efficient replication of hepatitis C virus. J. Virol. **82:**5761–5773.
58. **Zhu, S., W. Li, M. F. Ward, A. E. Sama, and H. Wang.** 2010. High mobility group box 1 protein as a potential drug target for infection- and injury-elicited inflammation. Inflamm. Allergy Drug Targets **9:**60–72.